& Punongbayan, R. S.) 545–571 (Univ. Washington Press, Seattle, 1996).
16. Palais, J. M., Kirchner, S. & Delmas, R. J. Identification of some global volcanic horizons by major element analysis of fine ash in Antarctic ice. *Ann. Glaciol.* **14,** 216–220 (1990).
17. Pyle, D. M. On the 'climate effectiveness' of volcanic eruptions. *Quat. Res.* **37,** 125–129 (1992).
18. McCormick, M. P., Thomason, L. W. & Trepte, C. R. Atmospheric effects of the Mt Pinatubo eruption. *Nature* **373,** 399–404 (1995).
19. Zielinski, G. A. *et al.* Climatic impact of the AD 1783 eruption of Asama (Japan) was minimal: evidence from the GISP2 ice core. *Geophys. Res. Lett.* **21,** 2365–2368 (1994).
20. Zielinski, G. A. *et al.* Assessment of the record of the 1982 El Chichón eruption as preserved in Greenland snow. *J. Geophys. Res.* **102,** 30031–30045 (1997).
21. Clausen, H. B. *et al.* A comparison of the volcanic records over the past 4000 years from the Greenland ice core project and Dye 3 Greenland ice cores. *J. Geophys. Res.* **102,** 26707–26723 (1997).
22. Cole-Dai, J., Mosley-Thompson, E. & Thompson, L. Annually resolved southern hemisphere volcanic history from two Antarctic ice cores. *J. Geophys. Res.* **102,** 16761–16771 (1997).
23. Briffa, K. R. *et al.* Fennoscandian summers from AD 500: temperature changes on short and long timescales. *Clim. Dyn.* **7,** 111–119 (1992).
24. Briffa, K. R., Jones, P. D. & Schweingruber, F. H. Tree-ring density reconstructions of summer temperature patterns across western North America since 1600. *J. Clim.* **5,** 735–754 (1992).
25. Scuderi, L. A. Tree ring evidence for climatically effective volcanic eruptions. *Quat. Res.* **34,** 67–86 (1990).
26. Filion, L., Payette, S., Gauthier, L. & Boutin, Y. Light rings in subarctic conifers as a dendrochronological tool. *Quat. Res.* **26,** 272–279 (1986).
27. Anonymous *Annáler* **6,** 493–494 (1400–1800).
28. Frisch, C. (ed.) *Joannis Kepleris Astronomi Opera Omnia* **2/3** (1856–1871).
29. Keen, R. A. Volcanic aerosols and lunar eclipses. *Science* **222,** 1011–1013 (1983).
30. Simkin, T. & Siebert, L. *Volcanoes of the World* 2nd edn (Geoscience Press, Tucson, 1994).
31. Pyle, D. M. The thickness, volume, and grainsize of trephra fall deposits. *Bull. Volcanol.* **51,** 1–15 (1989); Assessment of the minimum volume of tephra fall deposits. *J. Volcanol. Geotherm. Res.* **69,** 379–382 (1995).
32. Fierstein, J. & Nathenson, M. Another look at the calculation of fallout tephra volume. *Bull. Volcanol.* **54,** 156–167 (1991).

Acknowledgements. We thank G. Salas, P. Francis, S. Self and the Instituto Geofisico de Peru, particularly the late M. Chang, for their collaboration on this project; P. Mayewski, L. D. Meeker, S. Whitlow and M. Twickler for their work in producing the initial sulphate time series of the GISP2 ice core; M. Germani and J. Palais for their help with the GISP2 tephra studies; J. Fierstein, M. Nathenson and N. Adams for help and discussions about the volume estimates; the members of the GISP2 community for work in developing the chronology of the core; and the Science Management Office, Polar Ice Coring Office and 109th Air National Guard for logistical support. Funding for this work has come from Indiana State University, and the National Science Foundation Petrology and Geochemistry Program, Office of Polar Programs (GISP2 work), and Atmospheric Sciences Program. The manuscript has benefited considerably from thorough reviews by D. Pyle and P. Allard.

Correspondence and requests for materials should be addressed to S.L.d.S. (e-mail: gesilva@scifac.indstate.edu).

A one-million-year-old *Homo* cranium from the Danakil (Afar) Depression of Eritrea

Ernesto Abbate*, Andrea Albianelli*, Augusto Azzaroli†, Marco Benvenuti*, Berhane Tesfamariam‡, Piero Bruni*, Nicola Cipriani*, Ronald J. Clarke§, Giovanni Ficcarelli*, Roberto Macchiarelli‖, Giovanni Napoleone*, Mauro Papini*, Lorenzo Rook*, Mario Sagri*, Tewelde Medhin Tecle¶, Danilo Torre† & Igor Villa#

* *Dipartimento di Scienze della Terra, Università di Firenze, 50121 Firenze, Italy*
† *Museo di Storia Naturale, Sezione di Geologia e Paleontologia, Università di Firenze, 50121 Firenze, Italy*
‡ *Eritrea National Museum, Asmara, Eritrea*
§ *Palaeo-Anthropology Research Unit, Department of Anatomical Sciences, University of the Witwatersrand Medical School, Johannesburg 2193, South Africa*
‖ *Museo Nazionale Preistorico Etnografico 'L. Pigorini', Sezione di Antropologia, 00144 Roma, Italy*
¶ *Ministry of Energy, Water and Mineral Resources, Department of Mines, Asmara, Eritrea*
# *Mineralogisches Institut, Abteilung für Isotopengeologie, Universität Bern, Switzerland*

One of the most contentious topics in the study of human evolution is that of the time, place and mode of origin of *Homo sapiens*[1–3]. The discovery in the Northern Danakil (Afar) Depression, Eritrea, of a well-preserved *Homo* cranium with a mixture of characters typical of *H. erectus* and *H. sapiens* contributes significantly to this debate. The cranium was found in a succession of fluvio-deltaic and lacustrine deposits and is associated with a rich mammalian fauna of early to early-middle Pleistocene age. A magnetostratigraphic survey indicates two reversed and two normal magnetozones. The layer in which the cranium was found is near the top of the lower normal magnetozone, which is identified as the Jaramillo subchron. Consequently, the human remains can be dated at ~1 million years before present.

The cranium, two incisors and two pelvic fragments were recovered between 1995 and 1997 near the village of Buia, Eritrea, about 100 km south-south-east of Massawa in the Danakil Formation, which is more than 1,000 m thick. This unit, also known as the Red Series[4,5], crops out extensively in the Danakil Depression, a belt of pronounced lithospheric extension at the intersection of the Red Sea, the Gulf of Aden, and the East African rift systems[6] (Fig. 1). It consists mainly of siliciclastic continental deposits with intercalations of lava flows and tuff beds at different levels. A Miocene to Pleistocene age is commonly assumed[4,5,7,8], and from a chronological and palaeo-environmental point of view, this formation can be correlated with the well-known hominid-bearing Awash Group in Ethiopia[9].

We examined the upper 500-m-thick portion of the Danakil Formation that is composed of grey to whitish clayey silts and sands with small amounts of marls laid down in fluvio-deltaic and lacustrine environments (Fig. 2).

Ash layers containing biotite have been found in the lower portion of the section. An initial attempt to date a biotite bulk separate by $^{39}Ar/^{40}Ar$ failed because of xenocrystic contamination.

As well as freshwater gastropod and fish remains, a large amount of fossil bones were found along the entire Buia section, and five mammal-rich levels have been identified (Fig. 2). The third level from the base yielded *Homo* remains consisting of a nearly complete and undeformed adult cranium (UA 31) (Fig. 3), two pelvic fragments (UA 173), and two permanent lower incisors (UA 222 and UA 369).

In the *Homo*-bearing outcrop, silts and clays alternate with sands. The cranium and pelvic fragments come from the upper part of a layer of laminated silty clays 1.4 m thick. The UA 369 incisor was

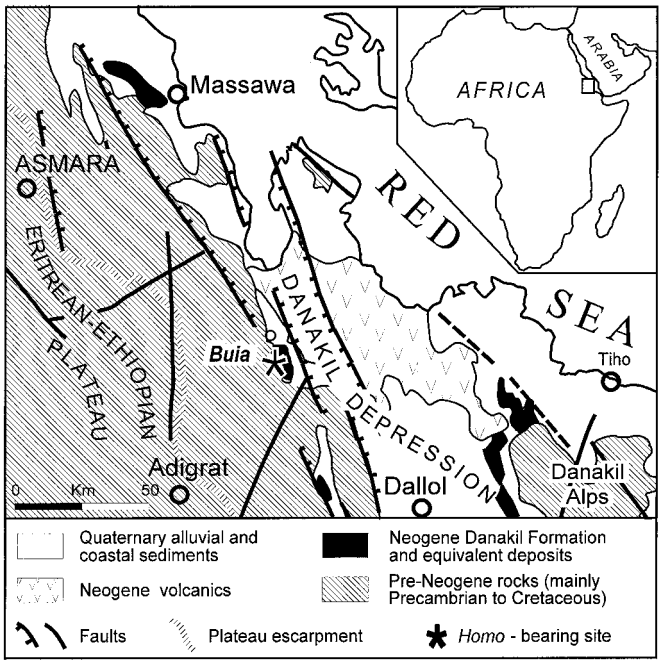

Figure 1 Simplified geology of the Northern Danakil Depression between the Eritrean-Ethiopian plateau and the Southern Red Sea. The palaeo-anthropological site near Buia is indicated by an asterisk.

found in a large sandy channel resting above this layer, and the UA 222 incisor comes from a thin lenticular sandy bed 1.5 m below the skull-bearing layer.

The *Homo*-bearing layer of the Buia section is exposed in several well-correlated outcrops in which a rich vertebrate fauna is represented by *Elephas recki, Hipparion* sp., *Equus* sp., *Ceratotherium simum,* Rhinocerotidae indet., *Pelorovis* sp., *Kobus ellipsiprymnus,* Bovidae indet., *Kolpochoerus* cf. *K. majus,* cf. *Kolpochoerus* sp. (advanced form), *Hippopotamus gorgops, Hexaprotodon karumensis,* Hyaenidae indet., Chelonia and Crocodilia. This is a typical African savanna fauna and indicates an age interval from early to early middle Pleistocene.

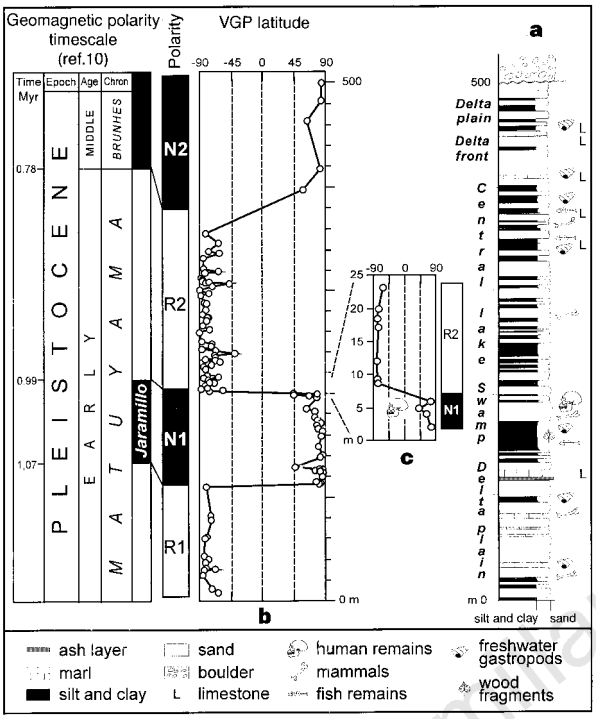

Figure 2 Stratigraphy of the Danakil Formation in the Buia area. **a,** Generalized lithostratigraphy with palaeo-environmental reconstructions. The boulder beds unconformably overlie the studied section. **b,** Composite magnetostratigraphic section obtained here and correlation with the Geomagnetic Polarity Time Scale. **c,** Detailed magnetostratigraphy of the site where the *Homo* cranium was found.

A magnetostratigraphic study was carried out on 97 hand samples collected in the silts and fine sands of the sequence. Characteristic directions of the palaeomagnetic vector, selected after thermal and alternative field cleaning procedures, yielded the virtual geomagnetic pole (VGP) latitudes used for defining the magnetostratigraphic succession (Fig. 2). Four magnetozones are recognized: two reversed R1 (0–115 m) and R2 (202–377 m), and two normal N1 (115–202 m) and N2 (377–500 m). The layer with the *Homo* remains is placed near the top of magnetozone N1.

On the basis of the biochronological and palaeomagnetic data, the Buia magnetozones have been correlated with the Geomagnetic Polarity Time Scale[10], and the magnetozone N1 has been identified as Jaramillo. This attribution relies on the following considerations. First, the mammal fauna gives a comprehensive age interval from the early Pleistocene to the early middle Pleistocene. Second, the succession does not reveal significant gaps and can be regarded as substantially continuous. Third, the two reversed magnetozones R1 and R2 are quite thick and, presumably, cover two relatively extended periods of time. They can be safely related to the Matuyama chron. Finally, the interposed polarity normal N1 has to be identified as Jaramillo, because it is thinner than the overlying N2. If N1 were identified as the Olduvai subchron, it would depend on the assumption that different intervals had markedly different rates of deposition, and there is no evidence for this. Because the *Homo*-bearing layer is near the top of the Jaramillo subchron it can be dated to ~1 Myr before present[10].

The cranium exhibits a nearly complete braincase (lacking most of the basicranium) and parts of the facial skeleton. No dental crowns remain, but the roots of the right P3, P4, M1, M2, M3 (mesial), and of the left P4, M1, and M2 are included in the alveoli.

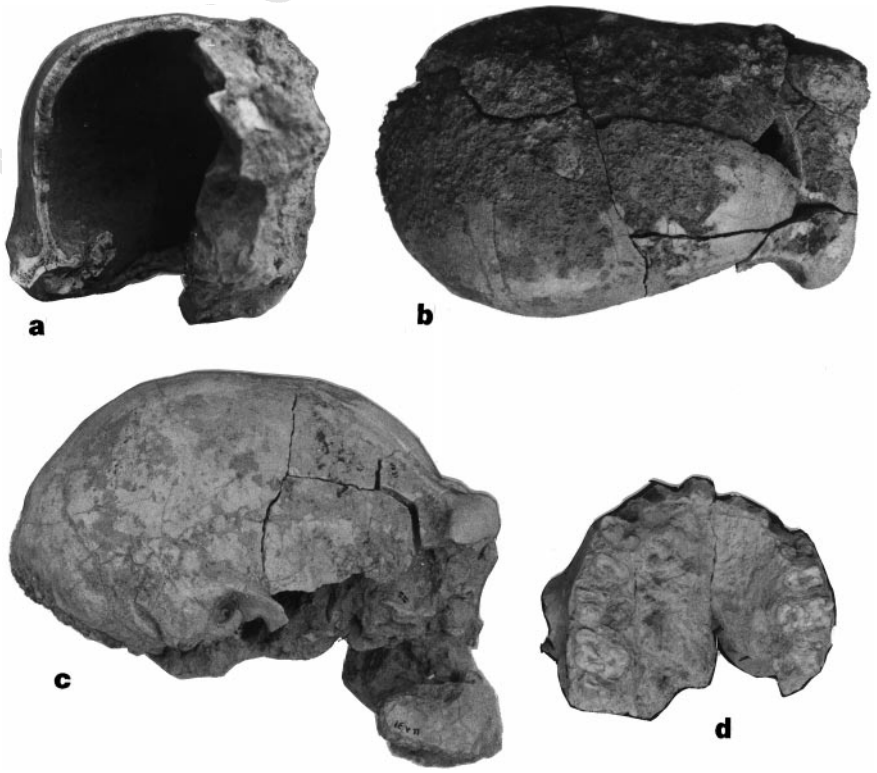

Figure 3 The UA 31 cranium. **a,** Frontal view of the braincase displaying a naturally exposed post-bregmatic coronal section through right parietal; **b**, upper view; **c**, right lateral view; **d**, basal view of the maxilla. (**a–c,** 30% of actual size; **d,** 60% of actual size).

A silty matrix still adheres to the external left half of the specimen.

For logistic reasons it has not yet been possible to clean, reconstruct and fully study the cranium, so here we offer only a preliminary assessment. For similar reasons the pelvic fragments and incisors are not described here.

A remarkable feature of UA 31 is its great anteroposterior length (204 mm) in relation to its maximum cranial breadth (130 mm). The greatest cranial breadth is located at the level of the supramastoid crests and with the length gives a cranial index of 63.7. Although the skull has not yet been restored and cleaned, tentative estimates suggest an endocranial capacity of 750–800 cm^3.

The neurocranium is low compared to its maximum length, but high relative to its transverse diameter. The upper-middle facial skeleton is slightly concave and marked prognathism is evident in the subnasal region. The face is narrow and short. The palate is shallow, wide and short, with its length reaching less than one-third of the total cranial length as seen in basal view. The very heavily built, forwardly projecting supraorbital torus is arched and thickened medially and over the middle of each orbit (17 mm). The minimum frontal breadth is 84.0 mm. Substantial elevation of the forehead and absence of sagittal keeling are evident in frontal view.

The frontal squame is well curved to bregma and the vault outline becomes gradually flatter on the parietals. The temporal lines originate in the form of a raised crest at the posterolateral margin of the supraorbital torus, but disappear early on the parietals. A slightly thickened angular torus is present. There is no nuchal torus, but a modest external protuberance is detectable where opisthocranion coincides with inion.

The specimen also shows a modest protrusion of the mastoid–supramastoid–auriculare complex lateral to the temporal squame. The mastoid process is short and broad. In coronal section, the parietal walls converge slightly inferiorly (Fig. 3); there is a high positioning of the maximum biparietal breadth (125.0 mm); the parietal thickness progressively decreases up to the midline (from 7.4 to 6.0 mm); the thickness at bregma is 6.3 mm.

The cranium from Buia shows the following combination of features, which are characteristic of the African specimens referred to *Homo erectus* and *Homo ergaster*[11,12]: long ovoid braincase with low endocranial capacity; greatest cranial breadth across the supramastoid crests; massive supraorbital torus; opisthocranion coincident with inion. One trait typical of *H. sapiens* is the high position of the greatest biparietal breadth with parietal walls converging slightly inferiorly. This mosaic of primitive and progressive features increases the known morphological variation reported for early–middle Pleistocene *Homo* crania and urges caution in the specific assessment of UA 31. Until we have conducted a full comparative study, we prefer to leave open its specific allocation.

Given its chronological position, in the middle of the time interval 1.4–0.6 Myr, from which no human cranial remains of comparable integrity are known from Africa[13], this unique Eritrean specimen provides a new perspective on the origins of modern humans. Its age indicates that morphology like that of *H. sapiens* had begun to differentiate in Africa at ~1 Myr, which is ~0.3 Myr earlier than previously estimated[1,2,14]. □

Received 25 September 1997; accepted 26 February 1998.

1. Bräuer, G., Yokoyama, Y., Falguères, C. & Mbua, E. Modern human origins backdated. *Nature* **386,** 337–338 (1997).
2. Ward R. & Stringer C. Molecular handle on the Neanderthals. *Nature* **388,** 225–226 (1997).
3. Bermúdez de Castro, J. M. *et al.* A hominid from the lower Pleistocene of Atapuerca, Spain: possible ancestor to Neanderthals and modern humans. *Science* **276,** 1392–1395 (1997).
4. Bannert, D. *et al.* Zür Geologie der Danakil Senke (Nördliches Afar Gebiet) NE Aethiopien. *Geol. Rundsch.* **59,** 409–443 (1970).
5. Brinckmann, J. & Kürsten, M. *Geological Sketchmap of the Danakil Depression* (Bundesanstalt für Bodenforshung, Hannover, 1970).
6. Barberi, F. & Varet, J. Volcanism of Afar: small-scale plate tectonics implications. *Geol. Soc. Am. Bull.* **88,** 1251–1266 (1977).
7. Merla, G. *et al. Geological Map of Ethiopia and Somalia 1:2,000,000 and Comment with a Map of Major Landforms* (Centro Stampa, Firenze, 1979).
8. Garland, C.R. *Geological Survey of Ethiopia Memoir* Vol. 1 (Berhanena Selam, Addis Ababa, 1980).
9. Kalb, J. E. *et al.* Geology and stratigraphy of Neogene deposits, Middle Awash valley, Ethiopia. *Nature* **298,** 17–25 (1982).
10. Berggren, W. A., Kent, D. V., Swisher III, C. C. & Aubry, M.-P. A revised Cenozoic geochronology and chronostratigraphy. *SEPM* (special publ.) **54,** 129–212 (1995).
11. Wood, B. *Koobi Fora Research Project* Vol. 4, *Hominid Cranial Remains* (Clarendon, Oxford, 1991).
12. Tobias, P. V. *Olduvai Gorge* Vol. 4, V-IX. *The Skull, Endocasts and Teeth of* Homo habilis (Cambridge University Press, 1991).
13. Wolpoff, M. H. *Human Evolution* (McGraw-Hill, New York, 1997)
14. Clark, J. D. *et al.* African *Homo erectus*: old radiometric ages and young Oldowan assemblages in the Middle-Awash valley, Ethiopia. *Science* **264,** 1907-1909 (1994).

Acknowledgements. All fossils are stored at the Eritrea National Museum, Asmara; inventory numbers refer to the provisional catalogue. We thank M. Pickford and T. D. White for discussions about the fossil record; M. R. Gibling, I. P. Martini, P. Passerini and A. Turner for critical reading of an earlier manuscript; A. Kibrab (Eritrea Department of Mines) and Y. Libsekal (Eritrea National Museum) for assistance in Eritrea; and F. Heller (ETH Magnetic Laboratory, Zurich). This work was supported by the Italian CNR (Cultural Heritage and TRANSRIFT projects), the PeriTethys Programme, the European Commission, the University of Florence, and the Italian Ministry for Foreign Affairs.

Correspondence and requests for material should be addressed to E.A. (e-mail: abbate@cesit1.unifi.it).

Selective foraging behaviour of basking sharks on zooplankton in a small-scale front

David W. Sims & Victoria A. Quayle

Department of Biological Sciences and Plymouth Environmental Research Centre, University of Plymouth, Plymouth PL4 8AA, UK

The basking shark *Cetorhinus maximus* is the second largest fish species, attaining lengths of up to 11 m. During summer months in temperate coastal waters circumglobally, these sharks filter-feed on surface zooplankton[1–4] near water-mass boundaries (fronts)[5,6]; however, little else is known about their biology[1]. Their foraging behaviour has not been investigated until now, although they have been described[2] as indiscriminate planktivores that are unlikely to orientate to specific plankton-rich waters. We have now tracked basking sharks responding to zooplankton gradients. We show that they are selective filter-feeders that choose the richest, most profitable plankton patches. They forage along thermal fronts and actively select areas that contain high densities of large zooplankton above a threshold density. They remain for up to 27 hours in rich patches that are transported by tidal currents and move between patches over periods of 1–2 days. We mapped feeding locations of these sharks in two years; the maps show that these sharks indicate broad shifts in front-located secondary production. Foraging behaviour of basking sharks therefore indicates the distribution, density and characteristics of zooplankton directly. This makes these sharks unique biological 'plankton recorders', with potential use as detectors of trends in abundance of zooplankton species that are influenced by climatic fluctuations of the North Atlantic Oscillation[7].

Natural foraging behaviour of filter-feeding marine fishes is poorly understood because of the problems associated with tracking them and quantifying food abundance simultaneously. However, the basking shark spends long periods feeding at the waters' surface, a behaviour that allows study of this shark by tracking, observation of active feeding, and sampling of zooplankton prey. During May–July in 1996 and 1997, we tracked visually the movements of aggregations of feeding sharks ($n = 13$ groups) and the fine-scale foraging movements of individual basking sharks ($n = 14$), and measured zooplankton density on their swimming paths off Plymouth, southwest England (50° 16 N 004° 09 W). We also recorded the positions of basking sharks sighted in addition to those tracked. During 1996 and 1997, we observed 58 and 54 different sharks, respectively.

Foraging locations of basking sharks seen during May–July in 1996–97 were orientated along a seasonal boundary separating coastal inshore water off Plymouth from fully stratified water of the